Interactions of fast C_{20} clusters with solids: Coulomb explosions, charge states and energy losses

2004 J. Phys.: Condens. Matter 16 1231

(http://iopscience.iop.org/0953-8984/16/8/008)

INSTITUTE OF PHYSICS PUBLISHING JOURNAL OF PHYSICS: CONDENSED MATTER

J. Phys.: Condens. Matter **16** (2004) 1231–1244 PII: S0953-8984(04)66498-8

Interactions of fast C_{20} clusters with solids: Coulomb explosions, charge states and energy losses

Hong-Wei Li[1], **You-Nian Wang**[1] **and Z L Mišković**[2]

[1] State Key Laboratory of Materials Modification, Department of Physics, Dalian University of Technology, Dalian 116023, People's Republic of China
[2] Department of Applied Mathematics, University of Waterloo, Waterloo, Ontario, N2L 3G1, Canada

E-mail: ynwang@dlut.edu.cn

Received 22 July 2003
Published 13 February 2004
Online at stacks.iop.org/JPhysCM/16/1231 (DOI: 10.1088/0953-8984/16/8/008)

Abstract

The dielectric response formalism is used to evaluate the dynamically screened interaction potential among the ions in a fast C_{20} cluster passing through a solid target. This potential is further used to calculate the individual ion charge states in the cluster by means of a statistical–variational theory which takes into account the effects of the vicinity of the neighbouring ions. Coulomb explosion and the energy losses of the cluster are simulated by solving equations of motion for individual ions while taking into account, in a self-consistent manner, the variation of ion charges in the course of explosion. Moreover, a Monte Carlo method is used to simulate the effects of multiple scattering of cluster constituent ions on target atoms. It is found that, owing to the wake-like asymmetry of the inter-ionic potential, both the distribution of ion charges in the cluster and the Coulomb explosion patterns exhibit strong spatial asymmetries in the direction of motion. It is also shown that the cluster energy losses exhibit characteristic interferences due to the vicinity effects, which diminish after long dwell times.

(Some figures in this article are in colour only in the electronic version)

1. Introduction

The interactions of energetic ion clusters with matter constitute a subject area of increasing interest due to its fundamental implications in physics and its potential in novel applications. Owing to their ability to deposit large amounts of energy in very small volumes of targets, fast cluster beams demonstrate a strong promise for use, for example, in materials modification and inertial confinement fusion. In particular, recent advances in accelerator techniques for the production of fast heavy clusters [1, 2] have provided a wealth of information on the morphology of track formation in solids. For example, it has been observed in a transmission electron microscope that MeV C_{60} clusters create long, amorphous and continuous tracks in

metals, insulators and semiconductors [3–6], which occupy cylindrical regions around the cluster paths, such that the latent radii of the tracks increase when the cluster energy increases.

Driven by the experimental advances, the need to understand the complexity of interactions of large clusters with solids has motivated a number of theoretical studies in recent years. The generally adopted scenario of cluster penetration through a solid target involves the initial stripping of the binding electrons of a cluster, after traversing just a few atomic layers, which triggers a Coulomb explosion of the cluster due to the dynamically screened inter-ionic interactions. Further penetration of the cluster is accompanied by intense electronic excitations of the target which exhibit strong interferences due to the spatial correlation among the ions, also known as the vicinage effect. In addition, for clusters made of heavier atoms such as carbon clusters, the effective charge states of the constituent ions also depend on the evolving cluster structure due to the vicinage effect, thus further complicating the dynamics of Coulomb explosion and the mechanisms of energy deposition in the target. On the other hand, for slower clusters made of lighter atoms, multiple scattering (MS) on target atoms may provide a supplemental mechanism of cluster break-up in solid targets, which sometimes can completely surmount Coulomb explosion. Such a complex scenario clearly indicates the need for a theoretical model which would treat the role of the vicinage effect in Coulomb explosion, energy losses and ion charge states in a self-consistent manner.

Over the past several years, significant progress has been achieved in theoretical work towards the development of such a model. Nardi and Zinamon [7] were the first to study Coulomb explosion of fast C_{60} clusters in solids by means of the molecular dynamics (MD) simulation, using a radially symmetric Yukawa-like interaction potential between the ions, which gave rise to expanding spherical-shell patterns. Very recently, those authors have extended their early work by considering the multiple scattering on target atoms and the charge-state evolution of the cluster constituent ions [8]. On the other hand, calculations of the dynamically screened self-energy of fast C_{60} clusters in solids showed that, owing to the wake pattern in the target dielectric response, the cluster structure could be stabilized against Coulomb explosion when the cluster size exceeds the characteristic length $\lambda_p = v/\omega_p$, where v is the cluster speed and ω_p is the plasma frequency of the electron gas in the target [9, 10]. In a recent work, motivated by this conclusion, MD simulations were used to reveal strong asymmetries in Coulomb explosion patterns of fast C_{60} clusters after long penetration times, which were attributed to the wake effects [11, 12], showing that the use of Yukawa-type interaction potentials may have limited applicability in studies of Coulomb explosions in solids.

Regarding the theoretical description of the vicinage effect on the charge state of partially stripped ions in fast clusters moving through solids, a model has been recently developed [13, 14] which combines the self-energy calculations [9] for atomic clusters in solids with the Brandt–Kitagawa (BK) theory [15] for the electronic structure of isolated heavy ions moving in solids. This model provides a self-consistent scheme to describe the influence of the surrounding ions on the effective charge state on each ion in the cluster. Such a model was used to describe the experimental data of Brunelle *et al* [16] on the dependence of the average ion charge on the number of constituent particles in carbon clusters passing through thin carbon foils. While the inter-ionic interactions were described by the Yukawa-type potential in those initial implementations of the model for the vicinage effect on ion charge states [13, 14], the recent application of this model to Coulomb explosions of swift diatomic molecular ions in solids has focused on the wake-potential asymmetry in the inter-ionic interactions and its effects on ion charge states [17].

The purpose of the present paper is to extend our previous work for diatomic molecular ions [17] to the case of larger clusters made of heavy atoms in order to elucidate the role of

the wake-potential effects in the cluster energy losses, the ion charge states and the Coulomb explosion patterns in a self-consistent manner, while taking into account the effects of multiple scattering. In section 2, we present the theoretical models used to determine the cluster self-energy, the ion charge states, the Coulomb explosions, the multiple scattering and the energy losses based on the dielectric response theory using the local-approximation dielectric function. The numerical results for fast C_{20} clusters in an Al target are presented in section 3, while a short summary is given in section 4. Atomic units (au) are used throughout, unless otherwise indicated.

2. Theoretical model

2.1. Self-energy and potential

Consider a homonuclear cluster with the atomic number Z entering a solid target with the velocity $\mathbf{v}$ oriented in the direction of the z axis. After passing through a few atomic layers, the cluster breaks up into n ions, which are placed at positions $\mathbf{r}_j$, with $1 \leqslant j \leqslant n$, in the laboratory frame. We consider relatively thin targets, such that the total energy losses of the cluster are negligible in comparison to its initial kinetic energy, allowing us to assume that the centre of mass (CM) of the cluster continues to move at the constant velocity $\mathbf{v}$. Moreover, since the cluster structure evolution during Coulomb explosion may be considered adiabatic when observed on the timescales of both the target electronic response and the charge-changing events, we neglect the change in the individual ion positions relative to the CM frame when calculating the dynamically screened inter-ionic interactions. Thus, the charge distribution of the cluster at time t is given by

$$\rho_{\rm ext}(\mathbf{r}, t) = \sum_{j=1}^{n} [Z\delta(\mathbf{r} - \mathbf{r}_j - \mathbf{v}t) - \rho_{e,j}(\mathbf{r} - \mathbf{r}_j - \mathbf{v}t)], \tag{1}$$

where $\rho_{e,j}(\mathbf{r} - \mathbf{r}_j - \mathbf{v}t)$ is the charge density of the electrons bound on the jth ion. In the BK theory [15], $\rho_{e,j}(\mathbf{r})$ is modelled by a radially symmetric function centred at the ion, as follows:

$$\rho_{e,j}(\mathbf{r}) = N_j \exp(-r/\Lambda_j)/(4\pi\Lambda_j^2 r), \tag{2}$$

where N_j is the number of the bound electron and Λ_j is the screening length of the ion.

The inter-ionic interactions within the cluster are described by the self-energy which is, within the framework of the dielectric response theory, given by [9]

$$E_{\rm s} = \frac{1}{2}\sum_{l=1}^{n}\sum_{j(\neq l)=1}^{n}\int \frac{{\rm d}\mathbf{k}}{2\pi^2}\frac{\rho_j(k)\rho_l(k)}{k^2\varepsilon(k, \mathbf{k}\cdot\mathbf{v})}{\rm e}^{{\rm i}\mathbf{k}\cdot\mathbf{r}_{jl}}, \tag{3}$$

where $\varepsilon(k, \omega)$ is the dielectric function of the medium, $\rho_j(k) = Z - N_j/[1 + (k\Lambda_j)^2]$ is the Fourier transform of the total charge density at the jth ion, $\rho_j(\mathbf{r}) = Z\delta(\mathbf{r}) - \rho_{e,j}(\mathbf{r})$, and $\mathbf{r}_{jl}$ is the relative position vector between the jth and the lth ions, $\mathbf{r}_{jl} \equiv \mathbf{r}_l - \mathbf{r}_j$. In general, the typical ion sizes Λ_j are much smaller than the inter-ionic distances $|\mathbf{r}_{jl}|$ within the cluster, so that equation (1) may be simplified by invoking the point-charge approximation, $\rho_j(\mathbf{k}) \simeq \rho_j(\mathbf{k} = \mathbf{0}) = Z - N_j$, as follows:

$$E_{\rm s} \approx \tfrac{1}{2}\sum_{l=1}^{n}\sum_{j(\neq l)=1}^{n}(Z - N_j)(Z - N_l)U(\mathbf{r}_{jl}), \tag{4}$$

where

$$U(\mathbf{r}_{jl}) = \frac{1}{2\pi^2}\int \frac{{\rm d}\mathbf{k}}{k^2}\frac{1}{\varepsilon(k, \mathbf{k}\cdot\mathbf{v})}{\rm e}^{{\rm i}\mathbf{k}\cdot\mathbf{r}_{jl}}, \tag{5}$$

is the dynamic interaction potential between two protons separated through $\mathbf{r}_{jl}$.

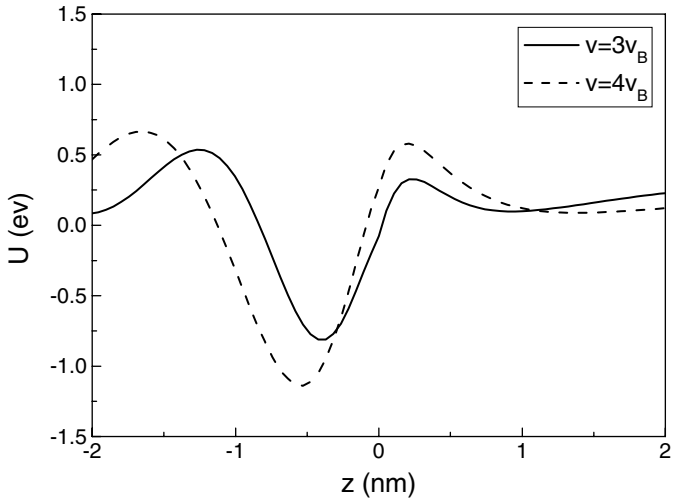

Figure 1. The dynamic potential $U(x, y, z)$ (in eV), equation (5), in an Al target as a function of the longitudinal distance z (in nm), with the transversal distances $x = y = 0.3$ nm, for two ion speeds, $v = 3v_B$ (full curve) and $4v_B$ (broken curve).

It is well known [18] that, for high-velocity ions, the potential $U(\mathbf{r}_{jl})$ has the form of an axially symmetric stationary wake cone trailing behind the ion, which can be represented by $U(\mathbf{r}_{jl}) = U_D(\mathbf{r}_{jl}) + U_W(\mathbf{r}_{jl})$, where $U_D(\mathbf{r}_{jl})$ is a symmetrically screened part of the potential and $U_W(\mathbf{r}_{jl})$ is the asymmetric part of the potential, i.e. the wake potential. In order to facilitate the numerical computations involving the interaction potential, we use in this work the local-approximation (LA) dielectric function [18]:

$$\varepsilon(k, \omega) = 1 - \frac{\omega_p^2}{\omega(\omega + i\gamma)}\Theta(k_c - k),$$

where $\omega_p = (4\pi n_0)^{1/2}$ is the plasma frequency of the electron gas with density n_0, γ is the damping factor, $k_c = \omega_p/v_F$ is a cut-off wavenumber with v_F being the Fermi velocity of the electron gas and $\Theta(x)$ denotes the unit step function. Using the LA dielectric function, one obtains the screened potential in cylindrical coordinates $\mathbf{r}_{jl} = \{\chi_{jl}, z_{jl}, \phi_{jl}\}$, as follows:

$$U_D(\mathbf{r}_{jl}) = \frac{1}{r_{jl}} - \frac{1}{\lambda_p}\int_0^\infty \frac{J_0(\kappa\chi_{jl}/\lambda_p)}{1+\kappa^2}\, e^{-\kappa|z_{jl}|/\lambda_p}\, d\kappa, \tag{6}$$

whereas the wake potential is given by

$$U_W(\mathbf{r}_{jl}) = \frac{2}{\lambda_p}\left[\int_0^{v/v_F} \frac{\kappa J_0(\kappa\chi_{jl}/\lambda_p)}{1+\kappa^2}\, d\kappa\right] \sin(z_{jl}/\lambda_p)\exp(\gamma z_{jl}/2v)\Theta(-z_{jl}), \tag{7}$$

where $\chi_{jl} = \sqrt{x_{jl}^2 + y_{jl}^2}$ and $\lambda_p = v/\omega_p$ is the screening length, while $J_0(x)$ is the zeroth-order Bessel function. Figure 1 shows the variation of the interaction potential $U(x, y, z)$ with the longitudinal distance z, for $x = y = 0.3$ nm, in an Al target. One observes that the dependence of the potential on z is rather asymmetric as a consequence of the wake effects in the spatial pattern of the medium's response.

2.2. Charge states

The total electronic energy of the cluster in the laboratory frame of reference consists of the kinetic energy of all bound electrons due to the cluster motion, the internal binding energies of electrons in individual ions and the self-energy taking care of the vicinage effect, namely [14]

$$E_{\mathrm{T}} = \sum_{l=1}^{n} N_l \frac{v_{\mathrm{r}}^2}{2} + \sum_{l=1}^{n} E_{\mathrm{is}}(N_l) + \frac{1}{2}\sum_{l=1}^{n}\sum_{j(\neq l)=1}^{n} (Z - N_l)(Z - N_j)U(\mathbf{r}_{jl}), \qquad (8)$$

where $v_{\mathrm{r}} = \langle|\mathbf{v} - \mathbf{v}_e|\rangle$ is the average speed of the cluster CM relative to the quasi-free electrons in the target [19] and $E_{\mathrm{is}}(N) = -(Z^2N^{1/3}/0.96)(1-N/(7Z))^2$ is the internal electronic energy of an isolated ion with N bound electrons [15]. Following the BK variational approach, the equilibrium charge states of the partially stripped constituent ions in the cluster can be determined from the following n coupled equations:

$$\frac{v_{\mathrm{r}}^2}{2} + E'_{\mathrm{is}}(N_l) - \sum_{j(\neq l)=1}^{n} (Z - N_j)U(\mathbf{r}_{jl}) = 0, \qquad (9)$$

for $1 \leqslant l \leqslant n$, where $E'_{\mathrm{is}}(N) \equiv \mathrm{d}E_{\mathrm{is}}/\mathrm{d}N$.

To simplify calculations, we assume in the following that the electron population N_l at the lth ion is close to the equilibrium number of bound electrons N_0 at an isolated isotachic ion, which is determined by solving the equation $v_{\mathrm{r}}^2/2 + E'_{\mathrm{is}}(N_0) = 0$. Thus, by expanding the function $E'_{\mathrm{is}}(N_l)$ in equation (9) about N_0 and keeping only the first-order terms, the numbers N_l of bound electrons at the constituent ions can be determined from the following n linear equations:

$$(N_l - N_0)E''_{\mathrm{is}}(N_0) - \sum_{j(\neq l)=1}^{n} (Z - N_j)U(\mathbf{r}_{jl}) = 0, \qquad (10)$$

where $E''_{\mathrm{is}}(N) \equiv \mathrm{d}^2E_{\mathrm{is}}/\mathrm{d}N^2$. We note that the error introduced in this approximation does not exceed a few per cent for inter-ionic distances greater than the typical equilibrium separations of atoms in a cluster. Figure 2 shows the velocity dependence of the charge $Q_0 = Z - N_0$ of an isolated carbon ion moving through an aluminium target.

2.3. Coulomb explosion

It is clear from equations (10) that each ion charge $Q_l = Z - N_l$ (with $1 \leqslant l \leqslant n$) becomes an implicit function, $Q_l = Q_l(\mathbf{r}_{jl})$, of all inter-nuclear relative positions $\mathbf{r}_{jl}$ within the cluster and is therefore expected to affect the Coulomb explosion dynamics. Coulomb explosion patterns can be obtained by solving the equations of motion where, for the lth ion, we have

$$\frac{\mathrm{d}\mathbf{r}_l}{\mathrm{d}t} = \mathbf{u}_l, \qquad (11)$$

and

$$m\frac{\mathrm{d}\mathbf{u}_l}{\mathrm{d}t} = F_{sl}(v)\mathbf{e}_z + \sum_{j(\neq l)=1}^{n} \mathbf{F}_{jl}(\mathbf{r}_{jl}, \mathbf{v}), \qquad (12)$$

where m is the ion mass, $\mathbf{u}_l$ is the ion velocity in the laboratory frame, while $F_{sl}(v)$ is the self-stopping force on the lth ion, given by

$$F_{sl}(v) = -\frac{2}{\lambda_{\mathrm{p}}^2}\int_0^{v/v_{\mathrm{F}}} \frac{\kappa\rho_l^2(\kappa)}{1+\kappa^2}\,\mathrm{d}\kappa \qquad (13)$$

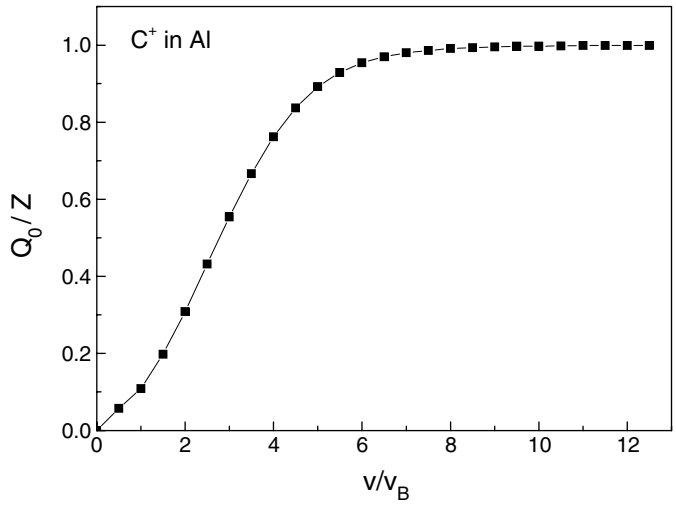

Figure 2. The charge state Q_0/Z as a function of the projectile velocity v (in au) for an isolated carbon ion moving through an Al target.

with $\rho_l(\kappa) = Z - N_l/[1 + (\kappa^2 + 1)(\Lambda_l/\lambda_p)^2]$ and $\mathbf{F}_{jl}(\mathbf{r}_{jl}, \mathbf{v}) = -Q_j Q_l \partial U(\mathbf{r}_{jl})/\partial \mathbf{r}_{jl}$ is the force exerted on the lth ion by the jth ion (with $j \neq l$). We have indicated explicitly that the forces in equations (11) and (12) depend on the velocity $\mathbf{v}$ of the cluster CM, but not on the individual ion velocities $\mathbf{u}_l$, owing to the adiabaticity of the Coulomb explosion. We note that the definition of the self-stopping force, equation (13), takes into account the charge distribution on the lth ion via the function ρ_l, while the inter-ionic forces $\mathbf{F}_{jl}$ are calculated in the point-charge approximation which is very accurate owing to the fact that $\Lambda_l \ll |\mathbf{r}_{jl}|$.

Figure 3 shows the dependences on z, with $x = y = 0.3$ nm, of the longitudinal and transversal components, F_z and F_y, of the interaction force $\mathbf{F}(x, y, z)$ between two protons moving through an Al target at equal velocities with a speed of $4v_B$, where v_B is the Bohr speed. We note that the oscillations in the magnitude of the force components shown in figure 3 are somewhat suppressed in comparison with those evaluated by Heredia-Avalos *et al* [12], presumably due to differences in the models of dielectric functions used in the two studies.

The equations of motion (11) and (12) can be solved numerically with the set of initial positions $\mathbf{r}_l(0) = \mathbf{r}_{j0}$ characterizing the equilibrium structure of the cluster, and with the initial velocities $\mathbf{u}_l(0) = \mathbf{v}$, neglecting the thermal vibrations of the constituent atoms.

2.4. Multiple scattering

Concomitant with the Coulomb explosion, the cluster also undergoes multiple scattering on target atoms. In the velocity range of interest here, the main effect of multiple scattering is to change the direction of individual ion velocities, whereas the nuclear energy loss is negligible in comparison to the electronic energy losses [19]. Therefore, one may expect that multiple scattering will contribute, in addition to the effect of Coulomb explosion, to a further overall increase of the inter-ionic separations in the course of penetration through the target.

For the sake of simulating multiple scattering, it is reasonable to assume that the cluster constituent ions are scattered independently from each other [10], and that each ion undergoes a random succession of binary collisions with the target atoms. We also assume that the multiple scattering is not affected by the variation of ion charge states in the course of penetration. We

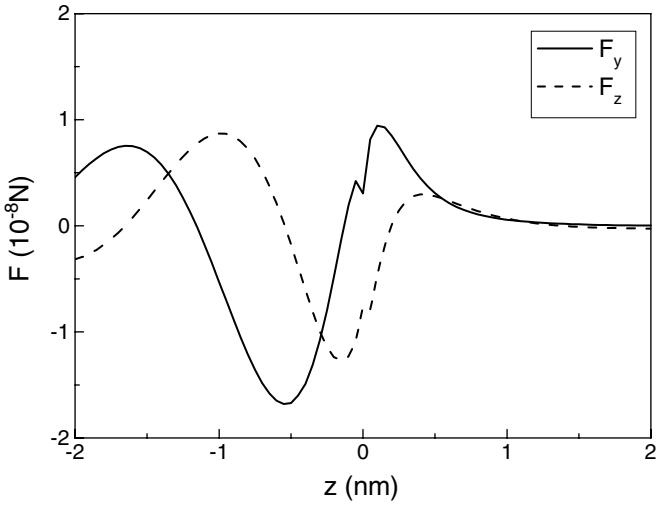

Figure 3. Components of the interaction force **F** between two protons moving through an Al target with equal velocities of $v = 4v_B$, at a relative position (x, y, z) from each other, with the z axis in the direction of motion. The dependences on z (in nm) of the longitudinal, F_z (broken curve), and the transversal, F_y (full curve), force components (in 10^{-8} N) are shown for $x = y = 0.3$ nm.

use here a Monte Carlo (MC) method to treat multiple scattering, which is based on the standard binary collision model [19]. During each time interval Δt, used to simulate the dynamics of Coulomb explosion, we generate a random free path for each ion in the cluster, $\lambda = -N^{-1/3} \ln R_1$, where R_1 is a uniform random number ($0 < R_1 < 1$) and N is the target atomic density, and compare it with the distance actually travelled by the cluster, $v\Delta t$. If $\lambda < v\Delta t$, the ion will be scattered; otherwise, no scattering takes place. The time interval Δt is chosen by using the procedure outlined in [8].

In the binary CM frame for an ion colliding with a target atom, the scattering angle θ_c is given by [20]

$$R_2 = \frac{\int_{\tau_{min}}^{\tau} d\sigma_n(\tau')}{\int_{\tau_{min}}^{\tau_{max}} d\sigma_n(\tau')}, \tag{14}$$

where R_2 is another uniform random number ($0 < R_2 < 1$), $\tau = \epsilon^2 \sin^2(\theta_c/2)$ is a dimensionless variable, ϵ is the reduced energy defined by

$$\epsilon = \frac{a_{TF} M_2}{Z Z_2 (m + M_2)} E, \tag{15}$$

with Z_2 and M_2 being the atomic number and the mass of the target atoms, respectively, and a_{TF} is the Thomas–Fermi screening radius, $a_{TF} = 0.885\,34(Z^{1/2} + Z_2^{1/2})^{-2/3}$. In equation (14), $d\sigma_n$ is the differential nuclear scattering cross-section, expressed as

$$d\sigma_n(\tau) = \pi a_{TF}^2 \frac{d\tau}{2\tau^{3/2}} f(\tau^{1/2}), \tag{16}$$

in terms of the universal screening function

$$f(\tau^{1/2}) = \lambda \tau^{1/2-\alpha} [1 + (2\lambda\tau^{1-\alpha})^{\beta}]^{-1/\beta}, \tag{17}$$

where λ, α and β are constants: $\lambda = 3.07$, $\alpha = 0.21$ and $\beta = 0.53$. The upper and lower integration limits in equation (14) are defined by $\tau_{max} = \epsilon^2$ and $\int_{\tau_{min}}^{\tau_{max}} d\sigma_n(\tau') = N^{-2/3}$. In

addition, the nuclear energy loss in the collision is given by

$$\Delta E_{\mathrm{n}} = \frac{4mM_2}{(m+M_2)^2} E \sin^2\left(\frac{\theta_{\mathrm{c}}}{2}\right), \tag{18}$$

where E is the ion kinetic energy.

According to the binary collision theory, the scattering angle in the laboratory frame is given by

$$\theta_{\mathrm{r}} = \arctan\left(\frac{\sin\theta_{\mathrm{c}}}{\cos\theta_{\mathrm{c}} + m/M_2}\right). \tag{19}$$

In the simulation, each constituent ion is followed with reference to a fixed axis, defined by the incidence direction of the cluster. After a collision takes place, the angle α with respect to this axis is determined by

$$\cos\alpha = \cos\alpha' \cos\theta_{\mathrm{r}} + \sin\alpha' \sin\theta_{\mathrm{r}} \cos\phi, \tag{20}$$

where α' is the angle before the collision, $\phi = 2\pi R_3$ is the azimuthal angle and R_3 is also a random number uniformly distributed between 0 and 1. Thus, after the collision, the ion velocity is given by

$$\mathbf{u} = \mathbf{u}' - \Delta\mathbf{u}, \tag{21}$$

where $\mathbf{u}'$ is the ion velocity before the collision and $\Delta\mathbf{u}$ is the change of the velocity, with

$$\begin{aligned} \Delta u_x &= \Delta u \sin\alpha \cos\phi, \\ \Delta u_y &= \Delta u \sin\alpha \sin\phi, \\ \Delta u_z &= \Delta u \cos\alpha, \end{aligned} \tag{22}$$

where $\Delta u = \sqrt{2M_2 \Delta E_{\mathrm{n}}/m^2}$. If a collision takes place, then the simulation of Coulomb explosion in the next time interval, based on equations (11) and (12), will start with the velocity $\mathbf{u}$, updated according to equations (21) and (22).

Thus, equations (10)–(22) constitute a self-consistent procedure to determine the evolution of ion charge states and the cluster structure due to Coulomb explosion and multiple scattering.

2.5. Energy losses

After determining the ion charge states and the evolution of cluster structure in the course of Coulomb explosion and multiple scattering, it is possible to deduce the time-dependent energy dissipation rate per unit path length or the stopping power, $S_{\mathrm{cl}}(v, t)$, for the cluster moving at the speed v. It can be shown that the stopping power can be expressed in terms of the force components in the direction of cluster motion, according to [21]

$$S_{\mathrm{cl}}(v, t) = S_0(v) + S_{\mathrm{v}}(v, t), \tag{23}$$

where

$$S_0(v) = -\sum_{l=1}^{n} F_{\mathrm{s}l}(v) \tag{24}$$

represents the contribution from the individual self-stopping forces, whereas

$$S_{\mathrm{v}}(v, t) = -\sum_{l=1}^{n} \sum_{j(\neq l)=1}^{n} (\mathbf{F}_{jl})_z(\mathbf{r}_{jl}, \mathbf{v}) \tag{25}$$

is the so-called vicinage stopping power which describes interferences in the energy losses due to the spatial correlation among the constituent ions.

Using the expression for the dynamic interaction potential, equation (7), it is straightforward to show that

$$S_{\rm v}(v,t) = \frac{2}{\lambda_{\rm p}^2}\sum_{l=1}^{n}\sum_{j(\neq l)=1}^{n} Q_j Q_l G(z_{jl}) \int_0^{v/v_{\rm F}} \frac{\kappa J_0(\kappa\chi_{jl}/\lambda_{\rm p})}{1+\kappa^2}\,{\rm d}\kappa, \tag{26}$$

with

$$G(z_{jl}) = \left[\cos\left(\frac{z_{jl}}{\lambda_{\rm p}}\right) + \frac{\gamma}{2\omega_{\rm p}}\sin\left(\frac{z_{jl}}{\lambda_{\rm p}}\right)\right]\exp\left(\frac{\gamma z_{jl}}{2v}\right)\Theta(-z_{jl}).$$

Here, it should be stressed that the time dependence of the stopping power comes from the time-dependent inter-ionic distances $\{\chi_{jl}(t), z_{jl}(t)\}$, as well as from the ion charges $Q_l(t)$, which also evolve with the cluster structure, as determined by equations (10)–(22).

3. Results for a C_{20} cluster

It is known [22, 23] that C_{20} is the smallest of all carbon fullerenes. In this paper, we choose C_{20} as a model cluster because, in Coulomb explosions, its equilibrium cage-like structure will be highly susceptible to any asymmetry in the inter-ionic interactions, as well as to the randomness of multiple scattering. Figure 4 shows several snapshots of the ion positions, obtained in simulations both (a) without and (b) with the effects of multiple scattering at times $t = 0$, 6, 12, 18 and 24 fs, for C_{20} clusters moving at the speed $v = 4v_{\rm B}$ through an Al target. It is interesting to notice that the C_{20} cluster structure evolves into a basket-like, or vase-like, shape, which becomes increasingly elongated in the direction of motion with increasing time as a direct consequence of the wake-potential asymmetry. Owing to the specifically chosen initial orientation of C_{20}, the patterns in figures 4(a) and (b) consist of four pentagons with different sizes, placed in the planes perpendicular to the direction of motion. Moreover, one can observe by comparing figure 4(a) with (b) that the longitudinal elongation of the cluster structure is somewhat reduced and the positions of the ions in each pentagon become slightly asymmetric in the presence of multiple scattering. It appears that the effect of multiple scattering is weak relative to the effect of Coulomb explosion. For example, after a penetration time of 24 fs, the longitudinal size of the cluster is about 4.5 nm when multiple scattering is taken into account, while this size is about 5 nm in the absence of multiple scattering.

In order to study the role played by the non-homogeneity of ion-charge distribution throughout the cluster, we show in figure 5 the results analogous to those in figure 4(b), but with all ion charges taken to be frozen during the cluster penetration and taken equal to the charge Q_0 of an isolated C ion moving at the same speed of $v = 4v_{\rm B}$. By comparison with figure 4(b), one finds that the cluster shape is somewhat broader in figure 5, indicating that the non-homogeneous charge distribution tends to hinder the cluster expansion in the lateral directions, but the effect does not appear to be too strong. In order to further reveal the asymmetry of the spatial distribution of ion charges due to the vicinage effect in the presence of wake interactions, we notice that, owing to both the axial symmetry of the interaction potential and the chosen orientation of the cluster, the groups of five ions in each of the four pentagons from figures 4 and 5 will have about the same charges. We show in figures 6(a) and (b) the time dependence of the ion charge ratio Q/Q_0 for C_{20} clusters moving through an Al target at the speeds $v = 3v_{\rm B}$ and $4v_{\rm B}$, respectively. In figures 6(a) and (b), the four curves labelled by A, B, C and D display the charge states of five ions in each of the four pentagons from figure 4(b), such that pentagon A is leading, whereas the curve labelled by E displays the average charge taken over all constituents in the cluster. Clearly, the vicinage effect on ion charges is quite pronounced in the early stages of Coulomb explosion, whereas the wake-potential asymmetry gives rise to a rather non-homogeneous distribution of ion charges. In particular, the ions in the

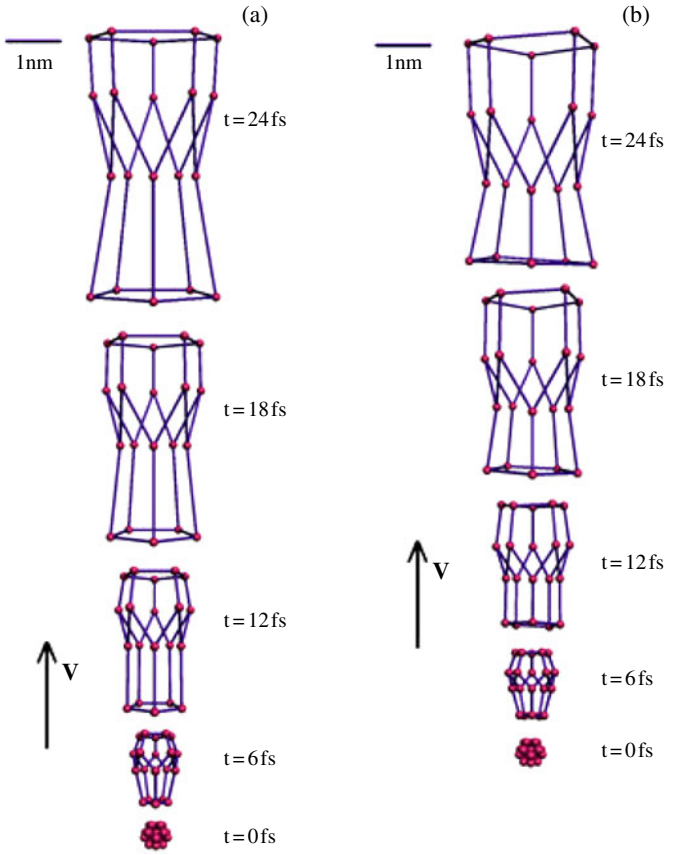

Figure 4. 3D Coulomb explosion patterns, obtained (a) without and (b) with multiple scattering (MS), for C_{20} moving through an Al target at the speed $v = 4v_B$ in the indicated direction. Snapshots of ion positions are given in a frame of reference attached to the cluster for several penetration times: $t = 0$, 6, 12, 18 and 24 fs.

leading pentagon A have a reduced charge state which increases towards Q_0 after prolonged times, whereas the initial charge reduction is less pronounced in pentagons B and C, which also pass through regions of increased charges, compared to Q_0, in the intermediate stages of Coulomb explosion. Interestingly, the ion charge in the trailing pentagon D is initially greater than Q_0 and, after passing through a maximum value, settles at Q_0 after long times. Finally, curves E in figure 6 show that the average charge is smaller than Q_0 at the initial stages of penetration, in accordance with the observations of Brunelle *et al* [16].

In order to elucidate the magnitude of the interferences in cluster energy losses due to the vicinage effect, we define the stopping ratio, $R(v, t) = 1 + S_v(v, t)/S_0(v)$, and display its dependence on the penetration time in figures 7(a) and (b) for C_{20} clusters moving at the speeds $v_0 = 3v_B$ and $4v_B$, respectively, through an Al target. In particular, we compare the results obtained in simulations with and without the effects of multiple scattering. It is seen that the energy losses are significantly enhanced due to constructive interferences at the early stages of Coulomb explosion and that R drops to a value close to 1 after some 5–10 fs, indicating a weakening of the vicinage effect due to the dispersion of the cluster. As expected, the effect of multiple scattering is to accelerate the reduction of the vicinage effect on energy losses, when compared to the case where only Coulomb explosion controls the dispersion of the cluster.

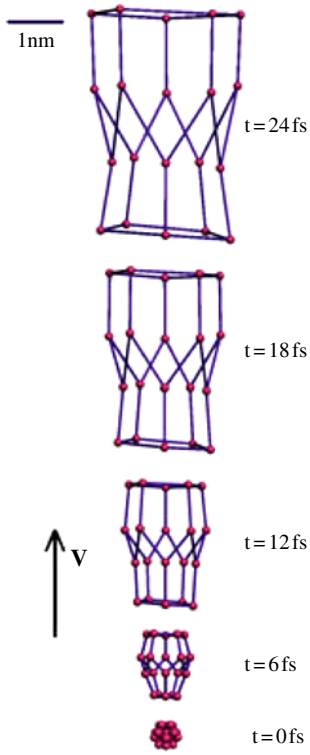

Figure 5. 3D Coulomb explosion patterns, including multiple scattering effects, for C_{20} moving through an Al target at the speed $v = 4v_B$ in the indicated direction. Snapshots of ion positions are given in a frame of reference attached to the cluster, for several penetration times: $t = 0$, 6, 12, 18 and 24 fs. Here, the ion charges are taken to be frozen at the value Q_0 of an isolated isotachic carbon ion.

4. Summary

We have presented a first version of a theoretical model for cluster penetration through a solid target by combining MD simulation of Coulomb explosion and MC simulation of the multiple scattering, which determines, in a self-consistent manner, all ion charges in the cluster for an instantaneous configuration of ions at any given moment of the penetration, and feeds back those charges into the equations of motion for Coulomb explosion. This dual self-consistency, involving the electron binding at the constituent ions as well as the dynamics of nuclear coordinates, is a unique feature of Coulomb explosions in matter, where the medium provides a dynamical and spatially anisotropic response to the group of spatially correlated ions. Namely, the dynamically screened potential in the medium is responsible for the ion motion in Coulomb explosion, the mutual influence of the constituent ions on each ion's ability to bind electrons, as well as for the deposition of energy into collective and single-particle excitations of the target electrons.

It is found that the wake-like asymmetry in the dynamic screening gives rise to rather strong effects in both Coulomb explosion and the ion-charge distribution. Whereas the magnitude of the vicinage effect on ion charges is quite strong in the initial stages of Coulomb explosion, when the ions are still close to each other, the wake asymmetry gives rise to a surprisingly non-homogeneous spread of ion charges throughout the cluster, such that the leading ions

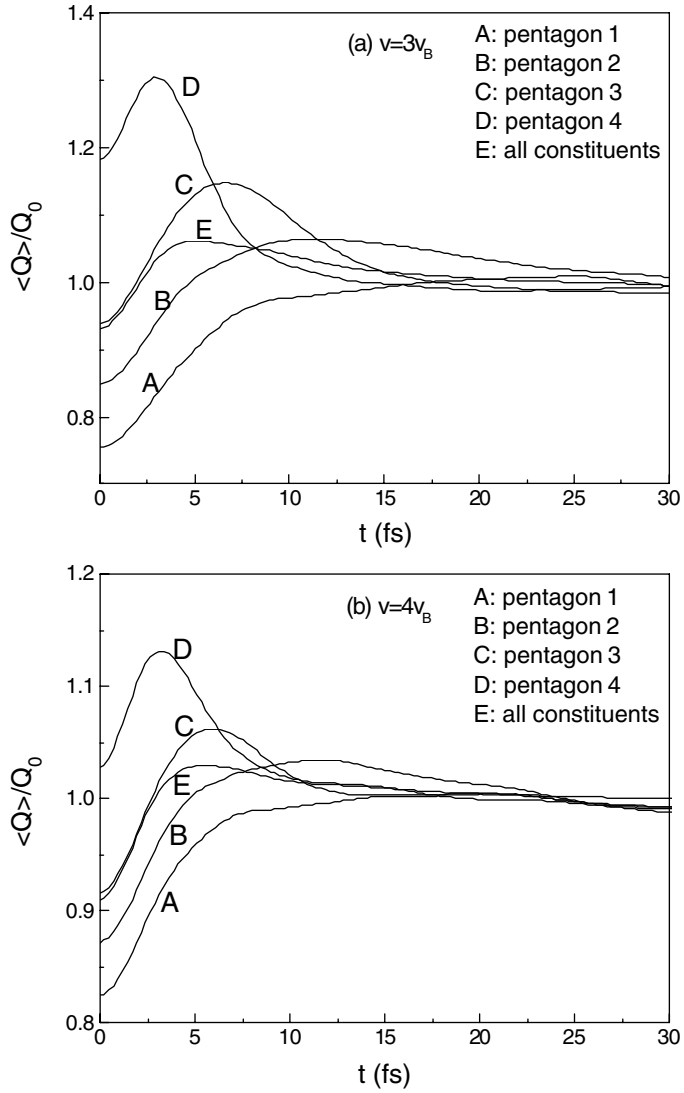

Figure 6. Charge state ratio Q/Q_0 for ions in C_{20} clusters moving through an Al target at two speeds: (a) $v = 3v_B$ and (b) $v = 4v_B$. The curves labelled by A, B, C and D display the charges of five ions in each of the four pentagons seen in figures 4 and 5, with pentagon A leading, whereas the curve labelled E displays the average charge taken over all constituents in the cluster.

appear with reduced charges, and the trailing ions with increased charges, as compared to the charge state of an isolated isotachic ion. The structure of the cluster appears to be generally growing in size in the course of penetration, while exhibiting pronounced elongation in the direction of motion of the cluster due to Coulomb explosion being driven by the inter-ionic potential with the wake asymmetry. On the other hand, the effects of multiple scattering are found to reduce this elongation and bring some asymmetry into the evolving shape of the cluster. Furthermore, the quantitative effect of the non-homogeneous distribution of ion charges is found to give rise to somewhat narrower cluster shapes, when compared to the penetration of the same cluster under the same conditions, but with the ion charges being

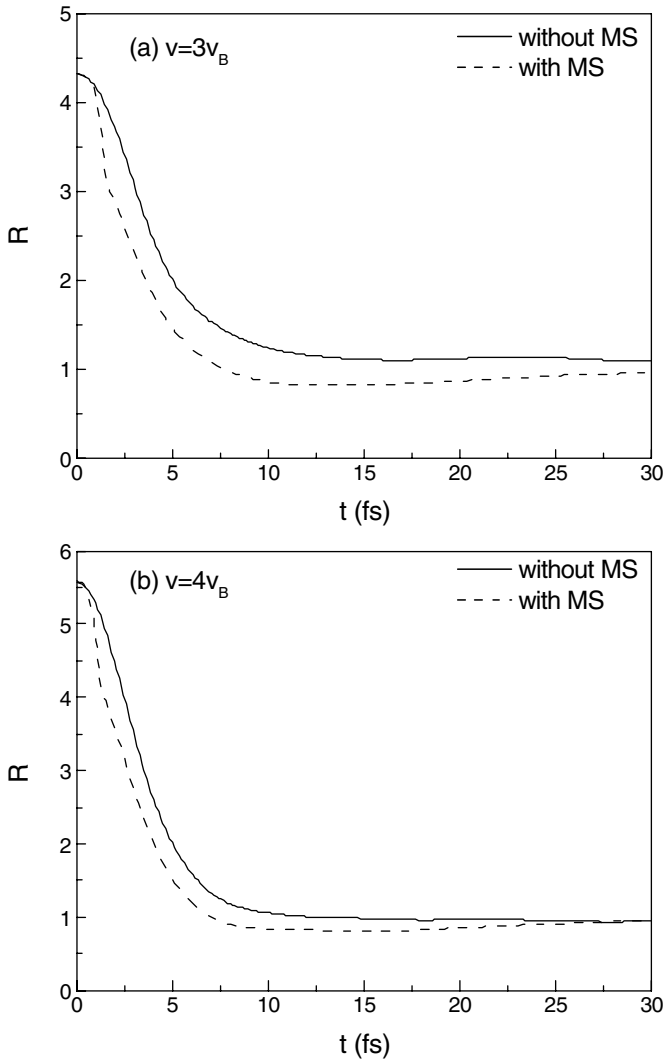

Figure 7. The stopping ratio $R = 1 + S_v/S_0$ versus the penetration time for C_{20} clusters moving through an Al target at two speeds: (a) $v = 3v_B$ and (b) $4v_B$, obtained without (full curves) and with (broken curves) multiple scattering.

frozen at the value for an isolated isotachic ion. Finally, the time dependence of the cluster stopping power is found to exhibit rather strong constructive interferences in the early stages of penetration, when the ions are still closely spaced, which diminish after sufficiently long time when the constituent ions fly apart. The variation and the non-homogeneous distribution of ion charge states are found to have relatively weak effects on the cluster energy losses, at least for the set of parameters used in the present simulations. On the other hand, multiple scattering clearly gives rise to a faster dispersion of the cluster, causing a quicker diminishing of the vicinage effect on the energy loss when compared to the simulation where multiple scattering is omitted.

The local-approximation dielectric function, used in the present work, has a rather limited range of applicability to sufficiently fast clusters, where long-ranged interactions and collective

electron excitations dominate the interactions with the target. A more elaborate dielectric function, including the dispersion and the local-field effects, will be used in future work, allowing a more appropriate description of interactions of slower clusters with solids.

Acknowledgments

This work is jointly supported by the National Natural Science Foundation of China (no 10275009) and the Grant for Striding-Century Excellent Scholar of Ministry of Education, State of China. ZLM acknowledges the support by the Natural Sciences and Engineering Research Council of Canada.

References

[1] Høakansson P, Della-Negra S, Mouffron J P, Waast B and Sullivan P 1996 *Nucl. Instrum. Methods Phys. Res.* B **112** 39
[2] Takahashi Y, Hattori T, Kashiwagi H, Hata T, Hayashizaki N, Sugai I and Noda K 2002 *Nucl. Instrum. Methods Phys. Res.* B **188** 278
[3] Dammak H, Dunlop A, Lesueur D, Brunnelle A, Della-Negra S and Le Beyec Y 1995 *Phys. Rev. Lett.* **74** 1135
[4] Dunlop A, Jaskierowicz G, Jensen J and Della-Negra S 1997 *Nucl. Instrum. Methods Phys. Res.* B **132** 93
[5] Jensen J, Dunlop A, Della-Negra S and Pascard H 1998 *Nucl. Instrum. Methods Phys. Res.* B **135** 295
[6] Ramos S M M, Bonardi N, Canut B, Bouffard S and Della-Negra S 1998 *Nucl. Instrum. Methods Phys. Res.* B **143** 319
[7] Nardi E and Zinamon Z 1995 *Phys. Rev.* A **51** R3407
[8] Nardi E, Zinamon Z, Tombrello T A and Tanushev N M 2002 *Phys. Rev.* A **66** 013201
[9] Mišković Z L, Liu W-K and Wang Y-N 1998 *Phys. Rev.* A **57** 362
[10] Mišković Z L, Liu W-K and Wang Y-N 1998 *Phys. Rev.* A **58** 2191
[11] Wang Y-N, Qiu H-T and Mišković Z L 2000 *Phys. Rev. Lett.* **85** 1448
Wang Y-N, Qiu H-T and Mišković Z L 2002 *Phys. Rev. Lett.* **88** 069901 (erratum)
[12] Heredia-Avalos S, Denton C D, Garcia-Molina R and Abril I 2002 *Phys. Rev. Lett.* **88** 079601
[13] Mišković Z L, Davison S G, Goodman F O, Liu W-K and Wang Y-N 2000 *Phys. Rev.* A **61** 062901
[14] Mišković Z L, Liu W-K, Goodman F O and Wang Y-N 2001 *Phys. Rev.* A **64** 064901
[15] Brandt W and Kitagawa M 1982 *Phys. Rev.* B **25** 5631
[16] Brunelle A, Della-Negra S, Depauw J, Jacquet D and Le Beyec Y 1999 *Phys. Rev.* A **59** 4456
[17] Li H-W, Wang Y-N and Mišković Z L 2002 *Nucl. Instrum. Methods* B **193** 204
[18] Echenique P M, Ritchie R H and Brandt W 1979 *Phys. Rev.* B **20** 2567
[19] Ziegler J F, Biersack J P and Littmark U 1985 *The Stopping and Range of Ions in Solids* vol 1 (New York: Pergamon)
[20] Adesida I and Karapiperis L 1982 *Radiat. Eff.* **61** 223
[21] Arista N 2000 *Nucl. Instrum. Methods Phys. Res.* B **164/165** 108
[22] Prinzbach H *et al* 2000 *Nature* **409** 40
[23] Ke X Z, Zhu Z Y, Zhang F S, Wang F and Wang Z X 1999 *Chem. Phys. Lett.* **313** 40